Steel and Composite Structures, Vol. 1, No. 2 (2001) 201-212
DOI: http://dx.doi.org/10.12989/scs.2001.1.2.201

Effect of loading rate on mechanical behavior of SRC shearwalls

Fumiya Esaki†

Department of Architecture, Faculty of Engineering, Kyushu Kyoritsu University, 1-8 Jiyugaoka, Yahatanishi-ku, Kitakyushu-City, Fukuoka, 807-8585, Japan

Masayuki Ono†

Department of Architecture, Kyushu School of Engineering, Kinki University, 11-6 Kayanomori, Iizuka-City, Fukuoka, 820-8555, Japan

Abstract. In order to investigate the effect of the loading rate on the mechanical behavior of SRC shearwalls, we conducted the lateral loading tests on the 1/3 scale model shearwalls whose edge columns were reinforced by H-shaped steel. The specimens were subjected to the reversed cyclic lateral load under a variable axial load. The two types of loading rate, 0.01 cm/sec for the static loading and 1 cm/sec for the dynamic loading were adopted. The failure mode in all specimens was the sliding shear of the in-filled wall panel. The edge columns did not fail in shear. The initial lateral stiffness and lateral load carrying capacity of the shearwalls subjected to the dynamic loading were about 10% larger than those subjected to the static loading. The effects of the arrangement of the H-shaped steel on the lateral load carrying capacity and the lateral load-displacement hysteresis response were not significant.

Key words: shear wall; loading rate; SRC edge column; sliding shear failure.

1. Introduction

According to the experimental studies on R/C monolithic framed shearwalls (hereafter referred to as "shearwall"), the two types of shear failure mode have been observed. One was the shear failure of edge columns. The other was the sliding shear failure of in-filled wall panel (hereafter referred to as "wall"). If the edge columns was sufficiently strong and properly reinforced, the shearwalls showed the sliding shear failure of their walls prior to the shear failure of their edge columns. This shear failure mode is allowable because the edge columns sustain the vertical load and consequently the pan cake crush of the building is prevented. It is effective to reinforce the edge columns with H-shaped steel in order to prevent their shear failure. In this paper, the effect of the loading rate on the mechanical behavior of shearwalls with edge columns where the H-shaped steel is arranged in the strong axis direction and in the weak one is discussed.

The cracking pattern, failure mode, lateral load-displacement hysteresis response and lateral load carrying capacity of framed shearwalls have been estimated by results derived from static loading tests. However, the mechanical behavior of shearwalls during an earthquake is expected to differ

†Professor

from the results in the static loading tests, since the structures are subjected to loading at higher speed during an earthquake.

According to the previous studies on the loading rate, the effects of the strain rate on the mechanical behavior of materials such as concrete and reinforcement steel bars, and the effect of the loading rate on the mechanical behavior of rod members such as reinforced concrete beams and columns have been investigated experimentally. The experimental studies concluded that the compressive strength and modulus of elasticity of concrete, and the yield strength of reinforcement bars increased in proportion to the logarithmic values of the strain rate, and also that the initial stiffness, cracking strength and lateral load carrying capacity of members increased as the loading rate increased (Iwai *et al.* 1972, Mogami and Kobayashi 1978 and 1979, Endoh *et al.* 1984, Mutsuyoshi *et al.* 1985, Hujii *et al.* 1986, Hujimoto *et al.* 1978-1991, Nakanishi *et al.* 1991). However, the experimental studies on the effect of the loading rate on the mechanical behavior of plate members such as shearwalls have been scarce. The effects of the loading rate on the mechanical behavior of shearwalls have been already discussed in the experiments on the 1/3 scale model of R/C shearwalls with opening conducted by the authors (Ono *et al.* 1998).

The aim of this study is to clarify the effects of the loading rate on the initial stiffness, cracking pattern, failure mode, lateral load-displacement hysteresis response, and lateral load carrying capacity of the shearwalls, and also to clarify the effects of the arrangement of the H-shaped steel in edge columns on the lateral load carrying capacity and the lateral load-displacement hysteresis response of the shearwalls.

2. Lateral loading tests

2.1. Specimens

The properties of test specimens and the mechanical properties of materials are summarized in Tables 1, 2 and 3, respectively. The nominal dimensions of specimens and the arrangement of the reinforcements are shown in Fig. 1. The specimens were designed so as to show the sliding shear failure of the wall prior to the flexural yielding at the critical section by using the equations which correspond to the failure modes (Esaki and Tomii 1982). However, the calculated lateral load carrying capacity dominated by the shear failure was only about 10% less than the calculated one dominated by the flexural yielding. The specimens were named “FdWt-L”, with “Fd” and “-L” denoting the direction of H-shaped steel and the loading rate, respectively. “Wt” denotes the thickness of the wall. “Fsx” and “Fsy” denote the specimens with the edge columns where the H-

Table 1 Properties of test specimens

Specimen	Arrangemnt of reinforcements in edge colum	Arrangement of wall reinforcement
Fsx W7-S Fsx W7-D Fsy W7-S Fsy W7-D	Longitudinal reinforcement: 4-D10 (p_g = 0.00713) Steel: H-100×50×5×7 ($_sp_g$ = 0.0296) Hoops: D6@70 mm (p_w = 0.00401)	D6@100 mm (p_s = 0.00401)

p_s = longitudinal reinforcement ratio, p_g = steel reinforcement ratio, p_w = hoop reinforcement ratio, p_g = wall reinforcement ratio

Table 2 Mechanical proper of reinforcement

Bar or Plate	a (cm^2)	σ_y (MPa)	σ_u (MPa)	E_s (GPa)	ε (%)
D6	0.281	407	546	164	22.8
D10	1.24	335	479	176	18.1
H-Shaped	0.821	412	475	186	26.5

a=cross sectional area, σ_y=yield strength, σ_u=tensile strength, E_s=Young's modulus, ε=elongation

Table 3 Mechanical properties of concrete

Specimen	σ_B (MPa)	${}_s\varepsilon_u$ (%)	E_s (GPa)
All	18.7	0.21	21.3

σ_B=compressive strength, ${}_s\varepsilon_u$=strain at peak stress, E_s=Young's modulus

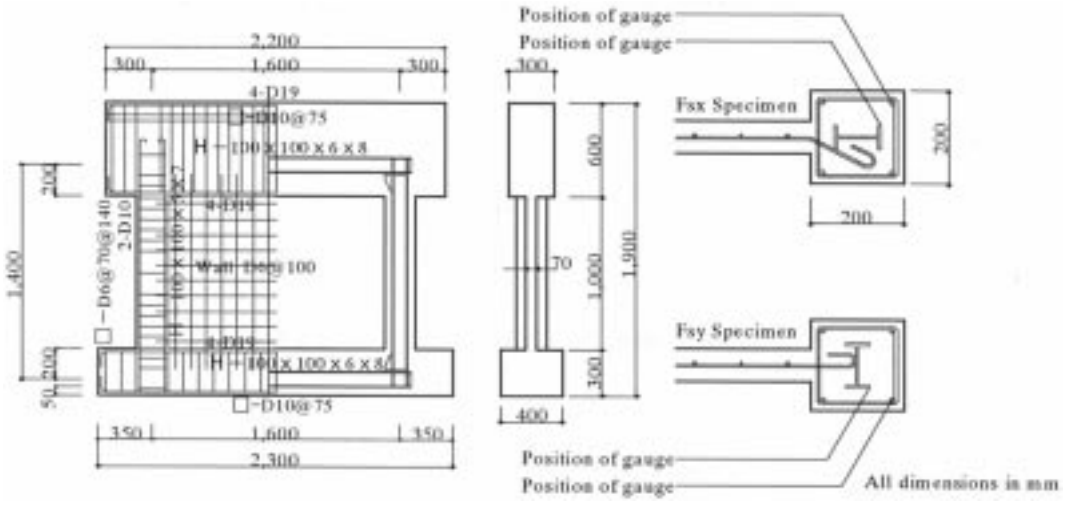

Fig. 1 Nominal dimensions and arrangement of reinforcement

shaped steel was arranged in the strong axis direction and in the weak axis one, respectively. "-S" and "-D" denote the specimens subjected to the static loading rate (= 0.01 cm/sec) and the dynamic loading rate (= 1 cm/sec), respectively. Though the loading rate applied to the shearwalls in existing buildings during earthquakes is expected to be higher than that adopted in these tests, the capacity of the loading machine available for use was a limiting factor which restricted loading rate in tests.

2.2. Loading apparatus and loading program

The loading apparatus is shown in Fig. 2. The lateral and vertical loads were applied to the specimens by the three actuators controlled by the electric computer. Two compressive vertical loads totaling 392 kN, were applied to the center of the left and center of the right edge columns by the two actuators. The vertical loads applied to the left and right edge columns were changed only by ΔN, which was the constant ratio to the lateral load, Q, so as to maintain the bending moment distribution of the specimens shown in Fig. 3. In these experiments, the vertical loads were changed so as to make the shear span ratio, $\alpha = Q/Ml$, to be 1.1, where Q and M were the maximum shearing force and bending moment and l was the distance between the center of the edge columns. The variable vertical load time hysteresis of the left and right actuators is shown in Fig. 4. The lateral load was controlled by the lateral displacement. The reversed cyclic load was applied to the specimens twice at each controlled displacement stage. The story

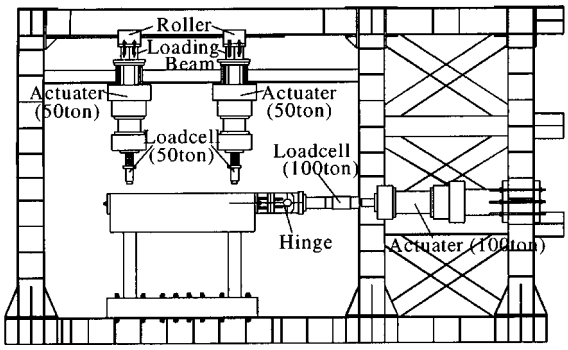

Fig. 2 Loading apparatus

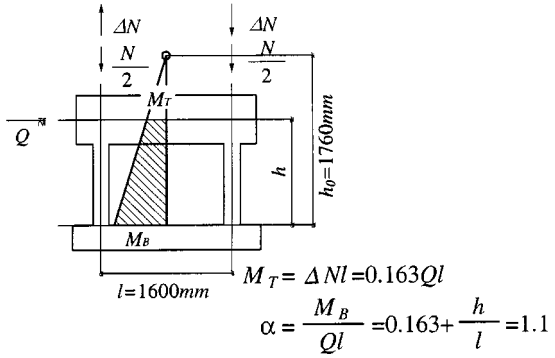

Fig. 3 Variable axial load and shear span ratio α

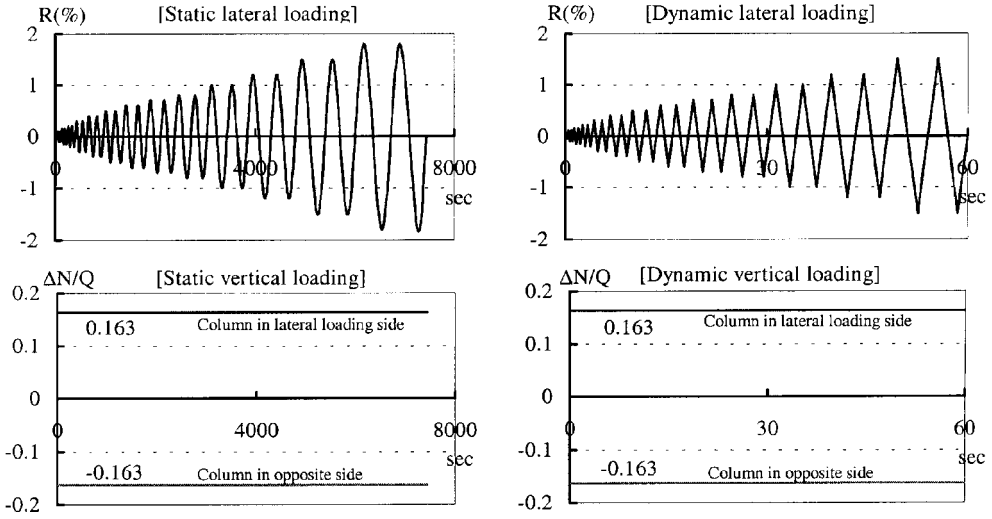

Fig. 4 Lateral and bertical loading programs

drift angle, $R=\delta/h$, was increased incrementally as shown in Fig. 4, where δ is the lateral displacement at the center of the upper beam and h is the story height from the upper side of the foundation beam to the position where the lateral displacement is measured.

2.3. Measurement system

The loads were measured by the load cells attached to the head of the actuators. As shown in Fig. 5, the displacements of the specimens were measured by the highly sensitive electric transducers attached to the steel frame fastened to the foundation beam of the specimens. The measured values were recorded on computer hard disks at each 0.4 sec for the static loading tests and 0.004 sec for the dynamic loading tests. The cracks were recorded on sketching, photograph, and video camera.

2.4. Test results

The relationships between the lateral load, Q, and the story drift angle, R, and the time hysteresis

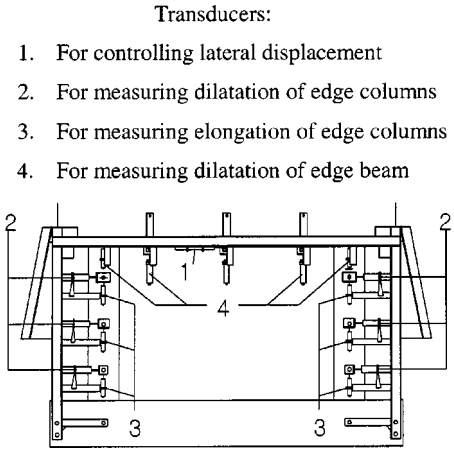

Fig. 5 Measurement system

of Q and R are shown in Fig. 6. The cracking patterns at the end of the tests are also shown in Fig. 6. Q_{max} denotes the maximum lateral load.

The cracking patterns and failure mechanism of the test specimens were as follows:

2.4.1. In the case of the static loading tests

The first shear cracking in the wall was observed at the controlled displacement stage of R = 0.15%. The shear cracking occurred continuously and extended as R increased. The horizontal cracking in the edge columns was observed at the controlled displacement stage of R = 0.2%. The sliding shear failure of the concrete in the wall panel occurred along the neighborhood of the bottom of the compression side edge column when R exceeded 0.6%. The sliding shear failure extended toward the center of the wall at the following cyclic loading stage. The crashing of the concrete and many shear cracks also occurred at the bottom of the compression side edge column. The maximum lateral load was reached at the controlled displacement stage of R = 1.2%. At the following cyclic loading stage, the lateral load dropped suddenly since the sliding shear failure of the concrete extended in the whole of the wall and the large shear cracking occurred at the bottom of the compression side edge column. However, the vertical load carrying capacity was maintained at the ultimate stage. The failure of the edge column reinforced by the H-shaped steel arranged in the weak axis was more severe than that in the strong one. However, the effects of the arrangement of the H-shaped steel on the lateral load carrying capacity and load-displacement hysteresis response were not significant. The H-shape steel was effective in preventing the shear failure and the deterioration of the vertical load carrying capacity in the edge columns.

2.4.2. In the case of the dynamic loading tests

The first shear cracking in the wall was observed at the controlled displacement stage of R = 0.05%. After the following cyclic loading stage, the shear cracking occurred continuously and extended itself, as the case of the static loading tests. The maximum lateral load was reached at the controlled displacement stage of R = 1.0%. After the following cyclic loading stage, the sliding shear failure occurred in the wall along the neighborhood of the bottom of the compression side edge column. The sliding shear failure extended toward the center of the wall at the following cyclic

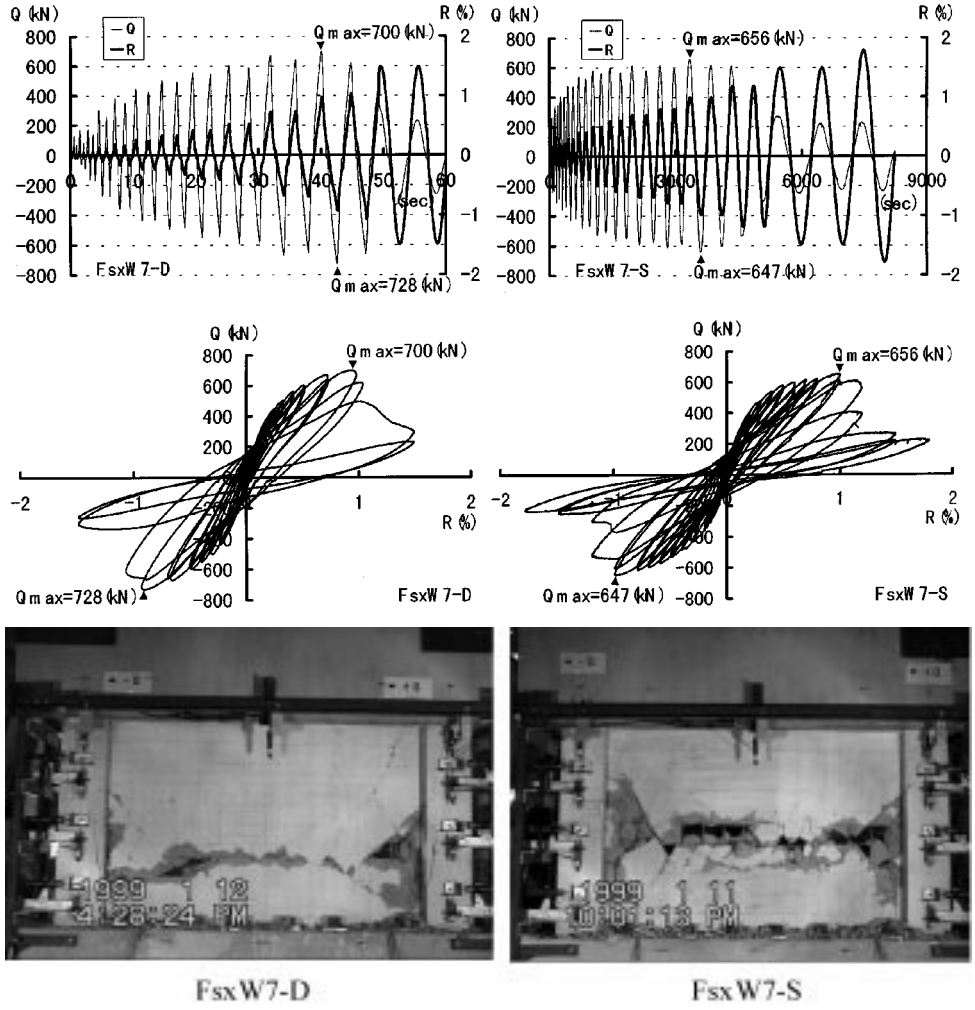

Fig. 6 (a) Lateral load, Q, -story drift angle, R, hysteresis response, Q and R time hysteresis and cracking pattern at ultimate stage in Fsx specimens

loading stage and, consequently, the lateral load dropped suddenly due to the sliding shear failure. The vertical load carrying capacity, however, did not deteriorate. If the sliding shear failure of the wall occurred prior to the other failure, it is necessary to make the shear strength of the ends of the edge column strong enough since the failure of the wall occurred during the short time in the dynamic loading tests and consequently the failure of the ends of the edge columns was more severe in the dynamic loading tests than in the static ones.

2.4.3. Effect of loading rate

The envelope curves of the load-displacement hystresis response are shown in Fig. 7. The initial lateral stiffness and load carrying capacity of the shearwalls subjected to the dynamic loading were about 10% larger than those subjected to the static loading. The story drift angle at the maximum lateral load in the case of the dynamic loading was smaller than that in the case of the static

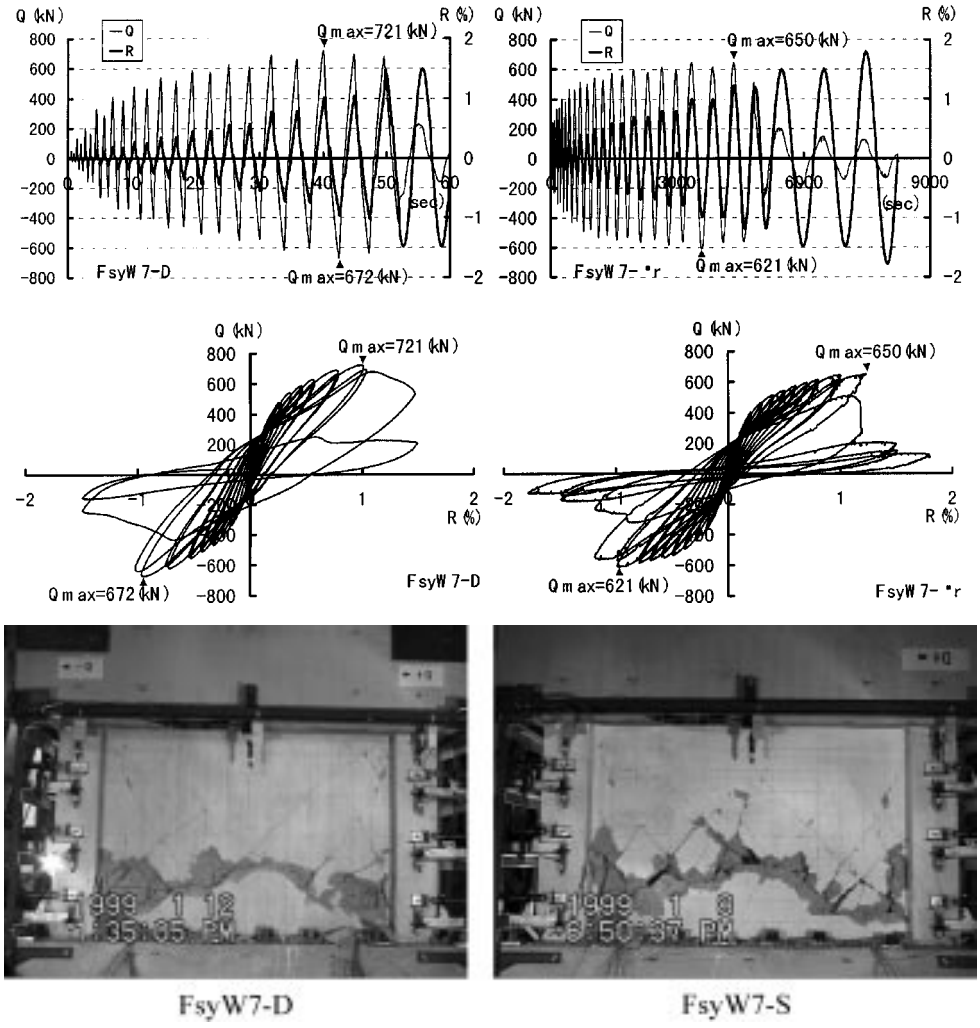

Fig. 6 (b) Lateral load, *Q*, -story drift angle, *R*, hysteresis response, *Q* and *R* time hysteresis and cracking pattern at ultimate stage in Fsy specimens

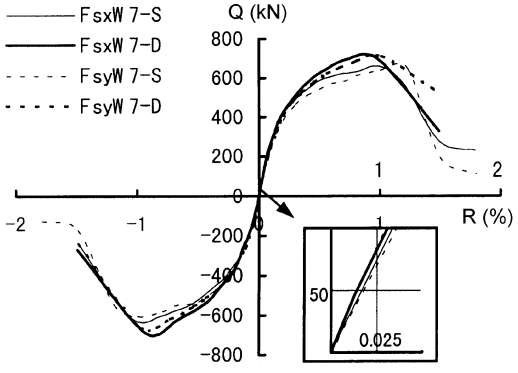

Fig. 7 Envelope curve of lateral load-story drift angle hysteresis response

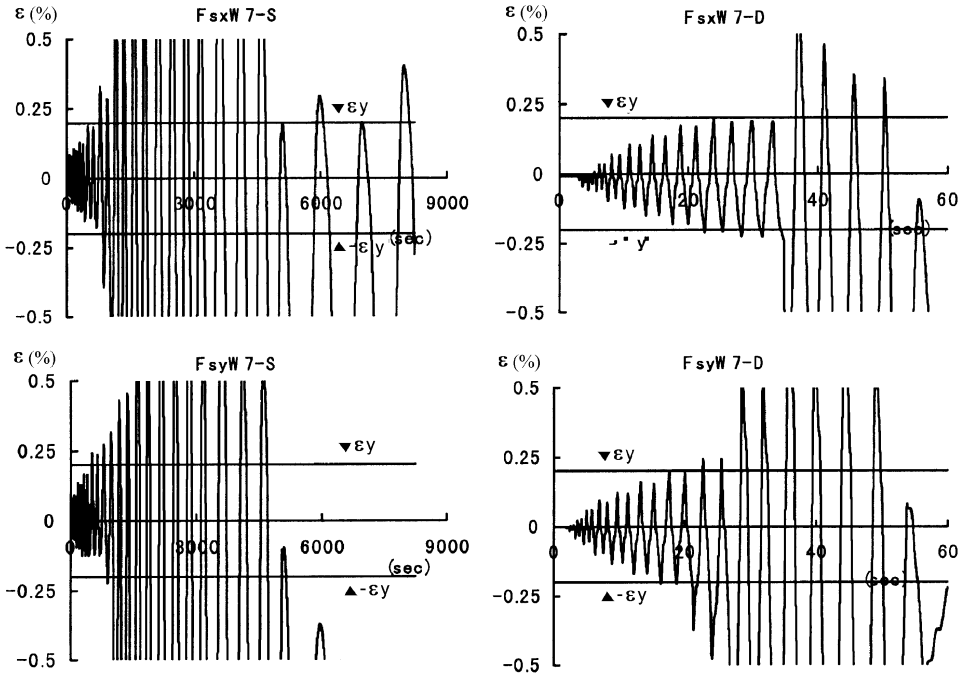

(1) longitudinal reinforcement bars

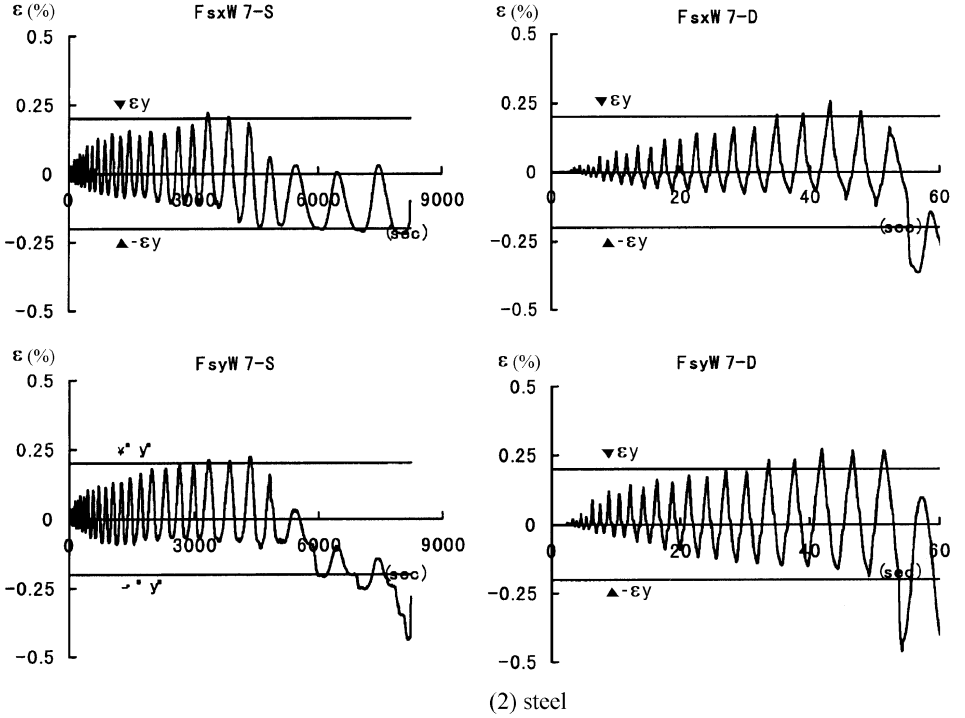

(2) steel

Fig. 8 Strain time hysteresis responses of longitudinal reinforcement bars and steel

loading. The dynamic increase factors of the compressive strength of concrete and yield strength of reinforcement bars were experimentally given by Eqs. (1) and (2), respectively (Nakamura *et al.* 1997 and Fujimoto 1988).

$$\frac{{}_D\sigma_c}{{}_s\sigma_c} = 1.59 + 0.224\log\dot{\varepsilon} + 0.021(\log\dot{\varepsilon})^2 \tag{1}$$

where,

${}_D\sigma_c$ = compressive strength of concrete at strain rate of $\dot{\varepsilon}$
${}_s\sigma_c$ = compressive strength of concrete at static loading
ε = strain rate

$$\frac{{}_D\sigma_c}{{}_s\sigma_y} = 1.39 + 0.1577\log\dot{\varepsilon} + 0.01577(\log\dot{\varepsilon}) \tag{2}$$

where,

${}_D\sigma_y$ = yield strength of reinforcement steel bar at strain rate of $\dot{\varepsilon}$
${}_s\sigma_y$ = yield strength of reinforcement steel bar at static loading

The strain time hysteresis responses of the longitudinal reinforcement bars and H-shaped steel are shown in Fig. 8. The observed mean strain rates of the diagonal compressive concrete in the wall and the longitudinal reinforcement bars in the edge columns are summarized in Table 4. The dynamic increase factors calculated by the mean strain rate of diagonal compressive concrete are close to the increase rate of lateral load carrying capacity. As shown in Fig. 9, the dilatation rate of

Table 4 Observed mean strain rates of diagonal strut in wall and longitudinal reinforcement in edge columns

	Diagonal strut (μmm/mm/sec)	Logi. Rein. (μmm/mm/sec)	H-shaped steel (μmm/mm/sec)	Dynamic increase factor
Fsx W7-S	62	78	28	-
Fsx W7-D	2215	3549	1963	1.14
Fsy W7-S	58	70	15	-
Fsy W7-D	3420	3955	2475	1.17

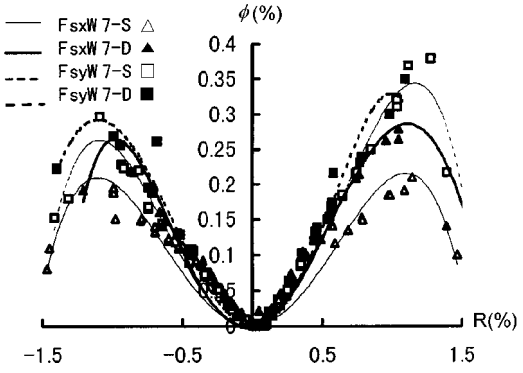

Fig. 9 Dilatation rate of area, Φ, and story angle, R relationship

Table 5 Summaries of test results and calculated values

Specimen	Observed values ${}_{ex}Q$ (kN)						Calculated values ${}_{cal}Q$ (kN), ${}_{ex}Q/{}_{cal}Q$				
	${}_{ex}Q_u$ (kN)		$\kappa_w \cdot {}_{ex}Q_u / (tl\sqrt{\sigma_B})$		${}_{ex}R_u$ (%)		${}_{cal}Q_{fu}$	${}_{cal}Q_{us1}$	${}_{cal}Q_{us2}$	${}_{cal}Q_{uws}$	${}_{cal}Q_{ucs}$
	+	-	+	-	+	-	781	515	499	740	1056
Fsx W7-S	656	647	1.58	1.56	0.979	0.980	0.840	1.27	1.31	0.886	0.621
Fsx W7-D	701	729	1.71	1.76	0.919	0.903	0.933	1.42	1.46	0.985	0.690
Fsy W7-S	650	621	1.57	1.50	1.230	0.965	0.832	1.26	1.30	0.879	0.616
Fsy W7-D	722	673	1.74	1.63	0.980	0.943	0.924	1.40	1.45	0.976	0.684

the area of the shearwall, $\Phi = \Delta S/S$, where ΔS is the increase of the area and S is the area of the shearwall prior to the loading tests, was larger in the dynamic loading specimens than in the static ones. This difference stems from the fact that the strength and stiffness of the materials are increased due to the effect of the loading rate.

3. Lateral load carrying capacity

The observed values of the lateral load carrying capacity, ${}_{ex}Q_u$, and the story drift angle at the peak lateral load, ${}_{ex}R_u$, are summarized in Table 5. The effects of the arrangement of the H-shaped steel on the lateral load carrying capacity and load-displacement hysteresis response were not statistically significant. The calculated values of the lateral load carrying capacity are also summarized in Table 5. ${}_{cal}Q_{fu}$ is the shear capacity dominated by the flexural failure (JSADP, 1992). ${}_{cal}Q_{us1}$ is the shear capacity calculated by the equation proposed in the Design Guidelines for Earthquake Resistance Reinforced Concrete Buildings based on the Ultimate Strength Concept (AIJ, 1990). ${}_{cal}Q_{us2}$ is the shear capacity calculated by the equation proposed by Hirosawa (Hirosawa M., 1975). ${}_{cal}Q_{uws}$ and ${}_{cal}Q_{ucs}$ are the shear capacity dominated by the sliding shear failure of the wall and by the shear failure of the edge column, respectively (Esaki *et al*. 1982). The longitudinal reinforcing bars in the edge columns yielded, but the steel did not yield at the peak lateral load.

The observed lateral load carrying capacity is close to ${}_{cal}Q_{uws}$. This fact holds true that the sliding shear failure of the wall occurred prior to the shear failure of the edge columns since the edge columns were reinforced with the H-shaped steel. As shown in Fig. 10, the lateral load carrying capacity of shearwalls which show this failure mode depends on the compressive capacity of the compressive struts formed in a cracked wall. The ultimate shear strength of the wall given by Eq. (3) was derived by the experiments of the concrete strut specimens subjected to the compressive and tensile loads at the same time (Esaki 2000). The observed ultimate shear strength ${}_{ex}\tau_u$ summarized in Table 5 was calculated by Eq. (4). In Eq. (4), κ_w is the shape factor for the shear stress at the center of the wall and is obtained by the I-shaped beam theory (Tomii 1957). It was indicated in the reference (Tomii and Hiraishi 1979) that the shape factor changed and because larger after the cracking than at an elastic stage. However, it is expected the redistribution of the shear stress occurs in some zones. In this investigation, the shape factor at an elastic stage was employed because of the reason mentioned above.

$$\tau_u = 1.85\sqrt{\sigma_B} \quad \text{(MPa)} \tag{3}$$

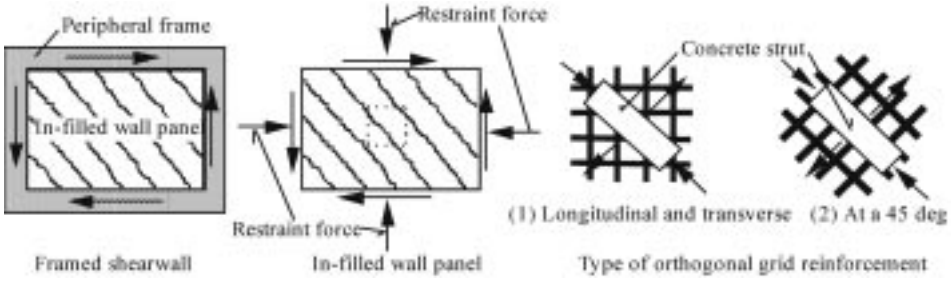

Fig. 10 Concrete struts formed in cracked wall of shearwalls and type of orthogonal grid reinforcement

where,

σ_B = compressive strength of concrete (Mpa)

$$_{ex}\tau_u = \kappa_w \frac{_{ex}Q_u}{tl} \tag{4}$$

where,

$_{ex}Q_u$ = observed lateral load carrying capacity (maximum lateral load)

t = thickness of wall

l = distance between center of edge column

The ultimate shear strength of the wall panel, $_{ex}\tau_u$, (observed at time of the sliding shear failure) is close to the shear strength obtained by the experiments of the concrete strut specimens (Esaki 2000). This fact indicates that the lateral load carrying capacity of the shearwalls failed in sliding shear can be predicted by the shear strength of the concrete struts obtained by the reference (Esaki 2000). The values of $_{ex}\tau_u$ are smaller than those by Eq. (3). This is due to the effect of the cyclic loading since the value was derived by the reversed cyclic loading tests, while Eq. (3) was derived by the monotonic loading tests.

4. Conclusions

In order to investigate the effect of the loading rate on the mechanical behavior of the shearwalls, the lateral loading tests on the 1/3 scale model specimens were conducted by adopting the two types of the loading rate which are $R = 0.0001$ rad/sec for the static loading and $R = 0.01$ rad/sec for the dynamic loading. The following conclusions reached as a result of the experiments:

1. The failure mode, predicted by the calculated lateral load carrying capacity, did not change in the range of the loading rate adopted in this tests.
2. The initial lateral stiffness and lateral load carrying capacity of the shearwalls subjected to the dynamic loading were about 10% larger than those subjected to the static loading.
3. The failure of the edge columns was more severe in the dynamic loading tests than in the static ones.
4. The lateral load carrying capacity recognized in the sliding shear failure of the wall can be estimated by the equations proposed in references (Esaki *et al*. 1988 and Esaki 2000).
5. The effects of the arrangement of the H-shaped steel on the lateral load carrying capacity and the lateral load-displacement hysteresis response were not significant.

Acknowledgements

Many students at Kyushu Kyoritsu University (KKU) and Kinki university assisted the experiments. Messrs. Tetsuo Kuriyama and Kenichi Hanada who are the technicians at KKU assisted the manufacture of the steel frame.

The authors thank all the people mentioned above for their contribution to this study.

References

AIJ. (1990), "Design guidelines for earthquake resistant reinforced concrete buildings based on ultimate strength concept", Architectural Institute of Japan, 122-135 (in Japanese).

Endoh, T. *et al.* (1984), "Experimental study on shear behaviors of reinforced concrete column components subjected to cyclic loading", *Proc. of JCI*, **6**, 689-692 (in Japanese).

Esaki, F. and Tomii, M. (1982), "Predicting method for shear failure modes of reinforced concrete framed shear walls", *Transactions of JCI*, **4**, 297-304.

Esaki, F. (2000), "Ultimate strength and strain of concrete struts in in-filled wall panels of framed shearwalls", *Proc. of 12WCEE*, Auckland, January, CD 0192.

Hirosawa, M. *et al.* (1975), "Comprehensive study on seismic performance of reinforced concrete shear wall", *Summaries of Technical Papers of Annual Meeting AIJ*, 1173-1174 (in Japanese).

Hujii, S. *et al*. (1986), "Effect of loading rate on behavior of R.C. column", *Summaries of Technical Papers of Annual Meeting AIJ*, August, 411-414 (in Japanese).

Hujimoto, M. *et al*. (1978-1991), "An experimental study of reinforced concrete column on high-speed loading, part 1-12", *Summaries of Technical Papers of Annual Meeting AIJ*, (in Japanese).

Fujimoto, M. *et al.* (1988), "Test of the single angle braces on high speed loading during an earthquake", *Transactions of AIJ*, No. 389, 32-41 (in Japanese).

Iwai, S. *et al.* (1972), "Effects of loading rate on the performance of structural elements", *Transactions of AIJ*, April, 102-111 (in Japanese).

Japan Society of Architectural Disaster Prevention (JSADP) (1992), "Standard for seismic evaluation of existing reinforced concrete buildings", *Japan Society of Architectural Disaster Prevention*, 11-12 (in Japanese).

Mogami, T. and Kobayashi, A. (1978), "Experimental study on strength and deformation of R/C beam subjected to high speed loading part 1 and 2", *Summaries of Technical Papers of Annual Meeting AIJ*, September, 1579-1580 (in Japanese).

Mogami, T. and Kobayashi, A. (1979), "Experimental study on strength and deformation of R/C beam subjected to high speed loading", *Summaries of Technical Papers of Annual Meeting AIJ*, September, 1293-1294 (in Japanese).

Mutsuyoshi, H. *et al.* (1985), "Behavior of reinforced concrete members subjected to dynamic loading", *Proceedings of JSCE*. No. 354/V-2, p. 81-90 (in Japanese).

Mutsuyoshi, H. *et al.* (1986), "Predicting the nonlinear earthquake response of reinforced concrete structures in consideration of strain rate effect", *Proc. of JSCE*, No. 366/V-4, 113-122 (in Japanese)

Nakamura, K. *et al.* (1997), "Experimental study of strain rate effects on reinforced concrete structure, part 1 and 2", *Summaries of Technical Papers of Annual Meeting AIJ*, September, 787-789 (in Japanese).

Nakanishi, M. *et al.* (1991), "Effect of loading speed on mechanical properties of reinforced concrete columns, part 1 and 2", *Summaries of Technical Papers of Annual Meeting AIJ*, September, 167-170 (in Japanese).

Ono, M. *et al*. (1998), "Effects of loading velocity on elasto-plastic behaviors of RC shear walls with an opening", *Proc. of JCI*, **20**(3), 595-600 (in Japanese).

Tomii, M. (1957), "Studies on shearing resistance of reinforced concrete plates", *Report of the Institute of Industrial Science University of Tokyo*, **6**(3), 1-45.

Tomii, M. and Hiraishi, H. (1979), "Elastic analysis of framed shear walls by assuming their infilled panel walls to be 45-Degree orthotropic plates, part 2 numerical examples", *Transactions of AIJ*, **284**, 51-61.

CC